International Symposium
On Turbulence and Shear Flow
Phenomena (TSFP-9)
June 30 - July 3, 2015 *Melbourne, Australia*

INNER–OUTER INTERACTIONS IN A TURBULENT BOUNDARY LAYER OVERLYING COMPLEX ROUGHNESS

Gokul Pathikonda
Mechanical Science and Engineering
University of Illinois at Urbana-Champaign

Kenneth T. Christensen
Aerospace and Mechanical Engineering; Civil & Environmental Engineering & Earth Sciences
University of Notre Dame
Notre Dame, Indiana, USA 46556
christensen.33@nd.edu

ABSTRACT

Hot-wire measurements were performed in turbulent flow overlying a smooth and a rough wall (the latter a multiscale topography) with the intent of investigating the details of inner–outer interactions. One-point measurements with a traversing probe were made to investigate the distribution of streamwise turbulent kinetic energy and large scale–small scale interactions at different regions of the smooth- and rough-wall cases. In addition, 2-probe simultaneous measurements were conducted and enabled investigation of inner–outer interactions wherein the large scales were always sampled in the outer layer. After identifying different regions across the boundary layer in the time-delayed correlation maps of the amplitude modulation coefficient, roughness-induced changes to the near-wall behavior were investigated. It was observed that the amplitude modulation influence on the near-wall small scales by the large scales in logarithmic region appears augmented in the rough-wall case compared to smooth-wall flow. Further, among the different spanwise positions investigated over the complex roughness (previously found to induce persistent secondary flows owing to spanwise heterogeneity of the topography), the low-momentum pathway region tended to have a 'stronger' interaction compared to the high-momentum pathway position.

INTRODUCTION

A smooth-wall turbulent flow at 'sufficiently' high Reynolds number (Re) can, broadly speaking, be divided into three regions: an inner, near-wall, turbulence-generating region, an outer wake region, and an inertial region in-between, where both the outer and inner scales are asymptotically and simultaneously valid. The turbulence-generating, near-wall region has first been experimentally observed as being populated by quasi-streamwise oriented vortices that form a self-sustaining turbulence generating mechanism (Kline *et al.*, 1967). These structures scale well with the inner scales of wall shear stress and viscosity. Hence, they had long been assumed to be independent of Re, mostly based on simple scaling arguments and the apparent invariance of the near-wall turbulent kinetic energy (TKE) peak in early hot-wire measurements and DNS simulations of such flows.

More recently, Kim & Adrian (1999) observed significant TKE content in the inertial region at much larger streamwise scales, and proposed a model of coherent very large scale motions (VLSMs, or superstructures). These superstructures were proposed to be trains of coherent vortex packets (termed *large scale motions, LSMs*), and their influence appeared in pre-multiplied spectral energy maps as a secondary TKE peak near the geometric center of the log region (Ng *et al.*, 2011), and at streamwise length scales $\sim O(10\delta)$ (Balakumar & Adrian, 2007), where δ is the outer length scale (the boundary layer thickness, pipe radius or channel half height). PIV measurements established the structural characteristics of LSMs (Christensen & Adrian, 2001), and the dynamic significance of these motions as influential contributors to local Reynolds shear stress (Ganapathisubramani *et al.*, 2003) and momentum transport (Natrajan & Christensen, 2006). Sufficiently long hot-wire rake measurements were made to establish the spanwise and streamwise characteristics of superstructures both statistically and instantaneously (Hutchins & Marusic, 2007), as they far exceeded the field of view of PIV measurements.

While the assumption of an independent near-wall turbulence cycle has been presumed, early observations by Rao *et al.* (1971) showed outer-scale influences indicating otherwise. More recently, Mathis *et al.* (2009) experimentally observed a clear amplitude modulation and superposition of the near-wall structures by the outer-scale superstructures, thus establishing a definitive interaction between the outer and inner regions of the flow that had previously been assumed to be decoupled (at least in a mean sense). This interaction was further modeled by Mathis *et al.* (2011), which correctly predicted many near-wall turbulence statistics. More recent studies on this phenomenon (Chung & McKeon, 2010; Ganapathisubramani *et al.*, 2012; Hutchins *et al.*, 2011) have attempted to establish the mechanism of these interactions in different regions of the flow. Ganapathisubramani *et al.* (2012)explored a similar interaction of frequency modulation between the small and large scales near the wall. These ideas are further elaborated on in the later sections of the current work.

Recently, interesting interpretations of the amplitude modulation analyses via two-point correlations and conditional averages have been explored. For example, Schlatter & Örlü (2010) showed that the amplitude modulation coefficient, as defined in Mathis *et al.* (2009), embodies contributions from the non-zero velocity skewness, and that the former and latter have a strong similarity–an observation also made in Mathis *et al.* (2009). Bernardini & Pirozzoli (2011) used DNS data to show that amplitude modulation is indeed a real interaction, though the coefficient defined by Mathis *et al.* (2009) includes contributions from skewness. Duvvuri & McKeon (2015) then established the phase interactions that occur in skewness and amplitude modulation coefficients for a turbulent velocity signal. More recently, Hutchins *et al.* (2011) revealed the 3D structure via conditional averaging, describing the various amplitude modulation effects. The strong relation between the gradient of large-scale velocity and the small-scale amplitude variations in the log region have been hypothesized as possibly due to meandering of the aforementioned superstructures in the spanwise direction.

The current work experimentally examines the strength and robustness of these interactions in rough-wall turbulent boundary layers. With the near-wall flow in smooth-wall turbulence replaced with a roughness-perturbed layer (termed the roughness sublayer), we aim to identify if and how superstructures in the log region of this rough-wall flow (identified in Mejia-Alvarez *et al.* (2014)) interact with the near-wall velocity perturbations within the roughness sublayer. Robustness of such interactions, or absence therein, would shed light on the possibility of using/modifying models developed for smooth-wall flow based on the amplitude modulation paradigm for rough-wall flows (including for near-wall modeling in LES of rough-wall turbulence, for example). The complex roughness used in the current study embodies a broad range of topological scales and induces spanwise-alternating, δ-scale, high- and low-momentum pathways (HMPs and LMPs, respectively; see Fig. 1), which have been well established as roughness-induced secondary flows in our previous work (Mejia-Alvarez & Christensen, 2013; Barros & Christensen, 2014).

EXPERIMENTS

All turbulent boundary layer experiments were conducted in an open-circuit, Eiffel-type, boundary-layer wind tunnel. Single-component constant temperature hot-wire measurements, made with a Dantec StreamLine 90C10 CTA system and 55P05 boundary-layer probes, are presented herein. The rough surface used for the rough-wall turbulent boundary layer experiments was the same as that originally fabricated and studied by Wu & Christensen (2007, 2010) and Mejia-Alvarez & Christensen (2010). Figure 1 shows the roughness topography in perspective view and further details about the topography, its manufacturing, the roughness physical characteristics, etc. can be found in Wu & Christensen (2007). The boundary layer under study was allowed to initially develop over the first 3 m of the smooth boundary layer plate, followed by an additional 3 m of development over the roughness. All measurements were conducted approximately 2.3 m downstream of the leading edge of the roughness. Wu & Christensen (2007) previously reported this rough-wall flow to have achieved self-similar conditions at this measurement location.

Two separate sets of measurements were performed for each case described in the current study: (1) with a single wall-normal-traversing probe (termed *1-Probe measurements* henceforth) and (2) with two identical probes at identical streamwise and spanwise positions making simultaneous measurements, with one probe fixed in log region and the other traversing from the wall towards the fixed outer probe (termed *2-Probe measurements*). Measurements were first performed for smooth-wall flow as a means of confirming and comparing the amplitude modulation effects with previous literature as well as a baseline against which the rough-wall data are compared. The single-probe measurements traversed the entire boundary layer, allowing all relevant scales of the flow to be determined (viscous velocity, u_τ, momentum deficit to roughness, ΔU, δ, U_∞, etc.). The two-probe measurements were then run at identical spanwise positions and at the same flow conditions, allowing one to assume the same flow parameters for both.

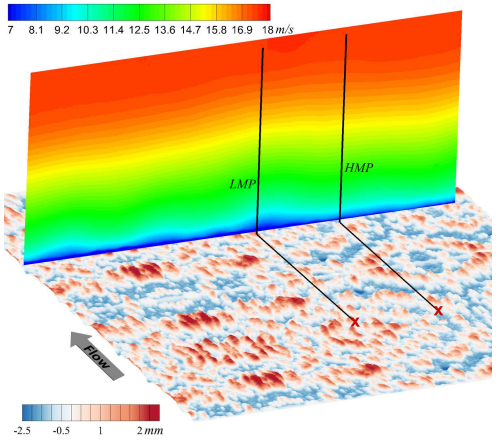

Figure 1. A to-scale schematic of the measurement locations with the roughness shown in perspective view. The mean streamwise velocity is presented in a cross-flow plane, highlighting the spanwise positions of the current measurements (denoted with 'X') at an LMP (*left*) and HMP (*right*) as previously identified by Barros & Christensen (2014). The current measurements were conducted 150 mm upstream of the cross-flow plane.

Table 1. Experimental parameters.

Flow	Re_τ	U_∞ (m/s)	δ_{99} (mm)	u_τ (m/s)	$y_\circ^+$
Smooth	3560	16.61	94.7	0.58	197 ($0.055\delta^+$)
R-LMP	5650	16.94	98.2	0.85	726 ($0.14\delta^+$)
R-HMP	4850	17.29	96.6	0.78	612 ($0.13\delta^+$)

Table 1 summarizes the parameters for the smooth- and rough-wall experiments conducted. The rough-wall measurements were conducted at distinct spanwise positions so that they resided at the spanwise position of an LMP and an HMP, as shown in Fig. 1. The flow parameters were extracted via parameter optimization by non-linear regression fit of the 1-Probe data to theoretical forms [composite function for smooth-wall flow, and Coles wake fit for rough-wall flow, as presented in Chauhan *et al.* (2007)]. All measurements were made at a sampling frequency of 70 kHz and a record length of 120 s per wall-normal position, giving a Nyquist frequency, $\Delta t^+ \sim 0.62$ (*superscript* '+' represents wall scaling), and a record length of $\sim 21{,}000\delta_{99}/U_\infty$.

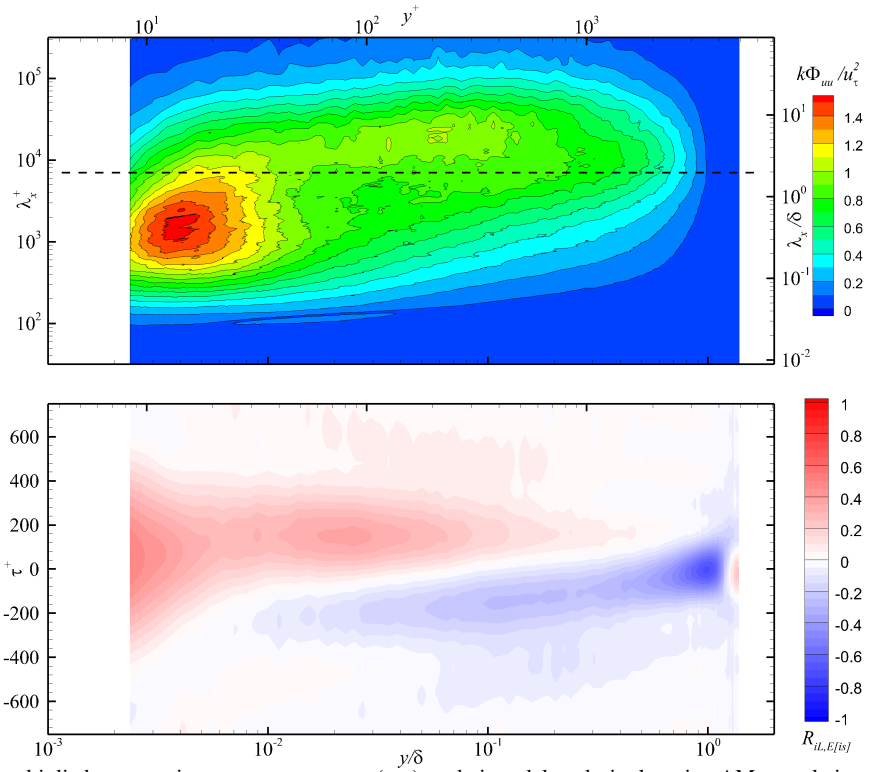

Figure 2. Pre-multiplied streamwise energy spectrum (top) and time-delayed single-point AM correlation (bottom) for smooth-wall flow. The dashed line corresponds to $\lambda_x^+ = 7000$ – the cut-off wavelength.

ANALYSIS

Profiles of mean streamwise velocity and streamwise TKE are not presented for brevity. Further, the reader is referred to Mathis *et al.* (2009) and Mathis *et al.* (2011) for a more detailed description of 1-probe and 2-probe analyses with respect to amplitude modulation. It should be noted that the 1-probe analysis correlates large-scale-amplitude (*envelope*) of small-scale velocity fluctuations ($E_L[u_i s^+](y^+)$) at a given location ('*inner*') with the large-scale velocity fluctuations at the same location ($u_{iL}^+(y^+)$). In the 2-probe analysis, the large-scale velocity fluctuations are taken at a fixed outer-layer wall-normal position ($y_\circ^+$). These latter analyses are particularly important in the rough-wall cases as the near-wall region is perturbed by a range of dynamically significant roughness length scales (Λ_L). Thus, 1-probe and 2-probe analyses are expected to show different trends in the rough-wall cases, in contrast to smooth-wall flow where previous studies have reported strong consistencies between 1-probe and 2-probe analysis.

Pre-multiplied streamwise energy spectra ($k_x\Phi_{uu}/u_\tau^2$) versus streamwise wavelength ($\lambda_x \equiv 2\pi/k_x$) are presented for all measurements, as they demarcate the distribution of streamwise TKE among logarithmically-spaced streamwise scales with wall-normal distance. The local mean velocity is used to convert the time scales into length scales. **Amplitude modulation (AM) correlation maps** are also presented in the current work, which are single-point (two-point, in case of 2-probe measurements) time-delayed velocity correlations (R) as a function of distance from wall, between the large-scale velocity fluctuations and the large-scale envelope of the small-scale velocity fluctuations (also shown in Jacobi & McKeon, 2013). The large and small scales are characterized by their wavelengths above and below the threshold of $\lambda_x^+ = 7000$, respectively, using an ideal filter (Mathis *et al.*, 2011). The convection velocity for the cut-off wavelength used is the local mean velocity for the 1-probe measurements and the mean velocity from the outer probe for 2-probe measurements.

RESULTS

1-Probe Analysis

Figure 2 presents the pre-multiplied streamwise energy spectrum and the 1-probe AM correlation maps for the smooth-wall flow, computed from the 1-Probe measurements. The pre-multiplied spectrum displays the expected inner and outer energy peaks near the wall and approximately at the geometric center of the log region, respectively. The horizontal line depicts the $\lambda_x^+ = 7000$ cut-off wavelength for the filter applied to compute the AM correlation map shown in Fig. 2. A positive time delay in the AM correlation maps ($\tau^+ > 0$) corresponds to a lead with respect to the large scales, and vice versa. The AM correlation map values at $\tau = 0$ with y correspond to the AM correlation coefficient variation reported in Mathis *et al.* (2009) and shown herein for smooth-wall flow in Fig. 3.

The correlation map shown in Fig. 2 can be viewed as reflecting the spatial structure of the small-scale amplitude fluctuations with respect to the large-scale fluctuations occurring at a given location represented by $\tau^+ = 0$ (Chung & McKeon, 2010; Hutchins *et al.*, 2011). The anatomy of such correlations can be divided into three distinct regions. First, the *outer peak* in the wake region in the vicinity of $y \sim \delta_{99}$ can be interpreted as reflecting entrainment of the free-stream fluid by the turbulent boundary layer, i.e., each time the probe senses an increased velocity (by the entrained fluid), simultaneous ($\tau^+ = 0$) decrease in small-

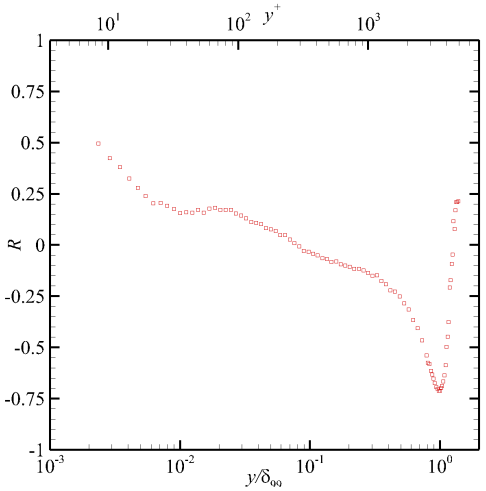

Figure 3. AM correlation coefficient, as defined by Mathis *et al.* (2009), with y.

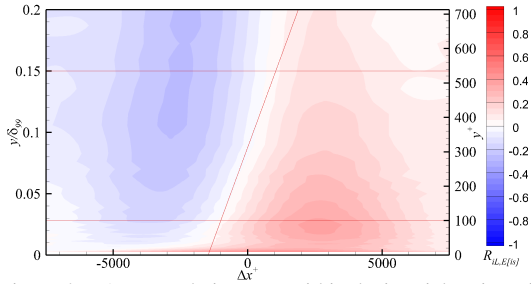

Figure 4. AM correlation map within the inertial region of smooth-wall flow. The two horizontal lines demarcate the approximate wall-normal bounds of the log region ($100y^* < y < 0.15\delta_{99}$). The 12° inclination is also highlighted.

scale fluctuations is observed, and vice versa. This has also been shown by Hutchins (2014) as the velocity skewness reflected in the AM correlation coefficient, and argued that this behavior is distinct from the AM that occurs closer to the wall. The *inertial region* show a symmetrically correlated–anti-correlated pair of small-scale amplitude fluctuations around the large-scale fluctuations, with a lead and a lag, respectively, relative to the large-scale fluctuations. Figure 4 shows that transforming the time delays into spatial information via Taylor's hypothesis using the mean velocity at the geometric center of the log region reveals this structure to be inclined at $\approx 12°$ in the streamwise direction. This structure angle is entirely consistent with that deduced from correlations of large-scale fluctuations near the wall and in the outer layer from the 2-probe measurements (not shown here for brevity). This behavior has also been reported in Chung & McKeon (2010) and Hutchins *et al.* (2011) via conditional averages that closely follow the gradient of the large-scale velocity fluctuations, and thus could be related to fluctuations in turbulence generation around the superstructures. As expressed by Hutchins (2014), the small scales could be 'preferentially arranged' around the large-scale structures in the log region, meaning that this behavior may not be AM phenomena. Finally, the *near-wall region* ($y/\delta_{99} < 10^{-2}$), clear AM of the small scales by the large scales is noted as a single correlation peak that is largest very close to the wall. This phenomenon

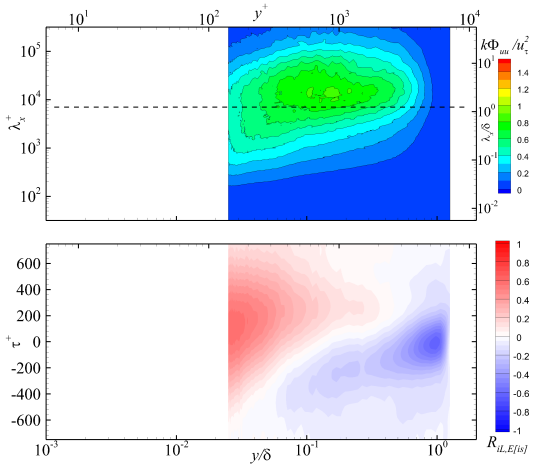

Figure 5. As in Fig. 2, but for rough-wall flow at a spanwise position coincident with an LMP.

has been interpreted by Hutchins *et al.* (2011) as a 'change' in the local Re that the inner region experiences when it is subjected to large-scale fluctuations from the outer flow.

With this interpretation of the base-state, smooth-wall flow in mind, Figs. 5 and 6 show similar 1-probe pre-multiplied streamwise TKE spectra and correlation maps for the rough-wall measurements at spanwise positions coincident with previously-identified LMPs and HMPs, respectively. Despite the near-wall region being perturbed by the complex roughness, the overall outer-layer structure is strikingly similar to smooth-wall flow. Though the inertial region in rough-wall flow does not exhibit the distinctive peaks observed in smooth-wall flow, the correlation–anti-correlation features are still present. This contrast is expected to grow with Re, as can be readily seen between the two spanwise positions with different 'local' Re. It is also noted that, in the 1-Probe measurements near the wall, the local large scales and the envelope of small scales still seem to correlate well. This observation is interesting because, within the roughness sublayer, one would expect structures on the scale of the roughness to perhaps dominate over any outer-layer interaction (or even between the large and small scales within the roughness sublayer for that matter). The presence of such interactions in the current results suggests the robustness of this phenomenon (at least for the spanwise positions presented). This observation also strengthens the view of the large-scale fluctuations imposing a changing Re effect on the inner region of the flow, to which the latter seem to continually adapt/react. However, it is anticipated that a 'sufficiently' strong roughness could still influence these interactions.

2-Probe Analysis

As mentioned earlier, the 2-probe measurements enable us to compare the influence of the large-scale fluctuations in the log region simultaneously on the small-scale fluctuations close to the wall. The pre-multiplied streamwise TKE spectra and the AM correlation maps are shown in Fig. 7 for smooth- and rough-wall cases. Here, the AM correlation maps represent two-point correlations computed between the large scales at a fixed location in the log layer and large-scale amplitude of the small scales near the wall. In this regard, the cut-off wavelength was maintained at $7000y^*$ for the 2-probe measurements and the outer-probe mean velocity was used for the Taylor's hypothesis recon-

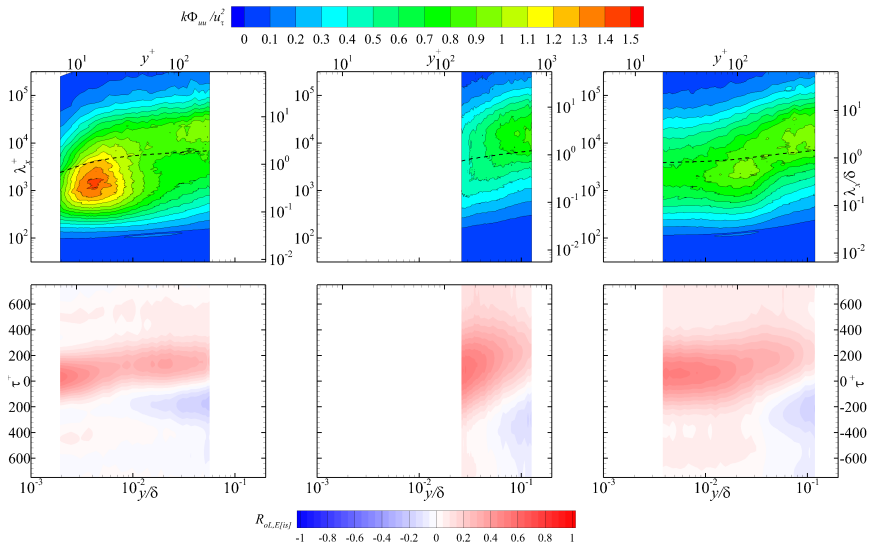

Figure 7. As in Fig. 2, but with 2-probe analysis. Left: Smooth; Middle: Rough (LMP); Right: Rough (HMP).

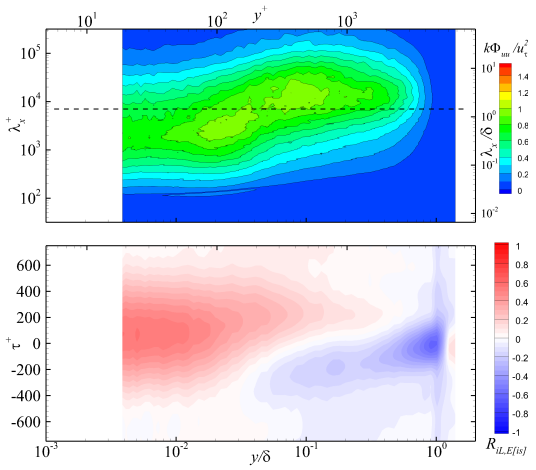

Figure 6. As in Fig. 2, but for rough-wall flow at a spanwise position coincident with a HMP.

struction. These measurements agree well with the 1-Probe measurements, with subtle differences. These measurements tend to contrast the near-wall and inertial region correlation behaviors more clearly, particularly in the smooth-wall case. This enhanced contrast, whereby the correlation–anti-correlation pair is enhanced in the 2-point correlations, is expected, particularly since the log region trends are interpreted as representations of a single superstructure (The difference in cut-off filter was confirmed to not be the reason for this trend).

Of particular interest, the 2-probe analysis allowed us to evaluate the efficacy of models representing these interactions, such as that proposed by Mathis *et al.* (2011) for smooth-wall flow, in a 'cause–effect' framework. The Mathis *et al.* (2011) model for this interaction assumes a *universal* small-scale signal ($u^*(y;y^*)$) close to the wall that is influenced by a log region fluctuation via a *linear superposition* and *amplitude modulation*. While details can be found in Mathis *et al.* (2011), the functional form for this model is given by

$$u_i^p = u^*(1+\beta u_{o,L}) + \alpha u_{o,L}, \qquad (1)$$

where $u_i^p(y;y^*)$ is the 'representative' inner velocity time series, $u^*(y;y^*)$ is the universal signal, $u_{o,L}(y_\circ/\delta)$ is the delay-adjusted outer large scales measured at $y = y_\circ/\delta$. In this framework, $\alpha(y)$ and $\beta(y)$ are *calibration constants*. With a set of 2-probe measurements with measured inner and outer scales, u^*, α and β can be estimated to 'predict' the near-wall signal for any single-point log region measurement made at the same log-layer position ($y_\circ/\delta$) and Re. In this context, α reflects the *strength of superposition* of outer large scales on the inner region, and β embodies the *strength of amplitude modulation* on the small scales close to the wall.

Both β and α were determined for the smooth- and rough-wall cases, and their variation with wall-normal distance in outer units is presented in Fig. 8. Both the α and β trends for smooth-wall flow match very closely those reported in Mathis *et al.* (2011). Below the inertial region, the maximum correlation between the large scales in rough-wall flow reduces more rapidly closer to the wall than it does in smooth-wall flow, as one might expect. However, the amplitude modulation, β, appears stronger in the rough-wall flow than the corresponding smooth-wall flow. In addition, flow along the LMP displays enhanced AM compared to the flow along the HMP.

SUMMARY

Amplitude modulation effects in a rough-wall turbulent boundary layer were explored using 1-probe and 2-probe hot-wire measurements. The 1-Probe measurements confirmed the expected TKE distribution in smooth-wall flow via the pre-multiplied energy spectra, and the inner–outer interaction mechanisms via AM correlation maps. Consistent with previous studies, the anatomy of small- and large-scale interactions locally and across the flow was observed in the smooth-wall results, including three different regions in the AM correlation map–the outer region, the inertial region, and the near-wall region. The present data and interpretation is consistent with that of Hutchins (2014), whereby 'true' amplitude modulation by the superstructures occurs only near the wall, in the inner region.

The rough-wall results show strikingly similar behavior in AM correlation maps, indicating that sustained AM effects survive roughness perturbations even within the roughness sublayer. This, though counter-intuitive, speaks

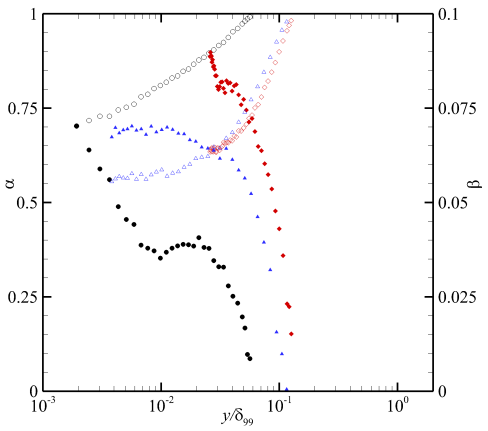

Figure 8. Variation of α (open) and β (solid) with y. ○: smooth; Δ: rough (HMP); ◇: rough (LMP).

to the potential robustness of such phenomena. It also adds to the interpretation by Hutchins *et al.* (2011) and Hutchins (2014) that AM of the inner region can be viewed as *a local and instantaneous change in Re that the sublayers experience and respond to, due to superstructures*.

The 2-probe measurements allowed the AM cause–effect relationships to be more directly investigated. Using the smooth-wall model proposed by Mathis *et al.* (2011), the strength of superposition and amplitude modulation were observed for the smooth- and rough-wall flows. The smooth-wall correlation maps bolstered the 1-Probe results and conclusions, agreeing with results reported in the literature (Mathis *et al.*, 2011). Not only were the inner–outer interactions found to survive the near-wall perturbations imposed by the roughness, but such effects were found to be even stronger in the rough-wall flows (as measured by β). Further, flow along LMPs seemed to have an enhanced AM effect on near-wall fluctuations than flow along HMPs. The superposition of outer large scales on near-wall small scales (as reflected in α), however, appear weakened in the rough-wall flow relative to smooth-wall flow, as one might expect.

ACKNOWLEDGEMENTS

This work is supported by the Air Force Office of Scientific Research under Grant No. FA9550-14-1-0101 (Dr. Rengasamy Ponnappan, Program Manager).

REFERENCES

Balakumar, B.J. & Adrian, R.J. 2007 Large-and very-large-scale motions in channel and boundary-layer flows. *Phil. T. Roy. Soc. A* **365** (1852), 665–681.

Barros, J.M. & Christensen, K.T. 2014 Observations of turbulent secondary flows in a rough-wall boundary layer. *J. Fluid Mech.* **748**, R1.

Bernardini, M. & Pirozzoli, S. 2011 Inner/outer layer interactions in turbulent boundary layers: a refined measure for the large-scale amplitude modulation mechanism. *Phys. Fluids* **23** (6), 061701.

Chauhan, K., Nagib, H. & Monkewitz, P. 2007 On the composite logarithmic profile in zero pressure gradient turbulent boundary layers. In *Proc. 45th AIAA Aerospace Sciences Meeting, Paper No. AIAA*, , vol. 532, pp. 1–18.

Christensen, K.T. & Adrian, R.J. 2001 Statistical evidence of hairpin vortex packets in wall turbulence. *J. Fluid Mech.* **431**, 433–443.

Chung, D. & McKeon, B.J. 2010 Large-eddy simulation of large-scale structures in long channel flow. *J. Fluid Mech.* **661**, 341–364.

Duvvuri, S. & McKeon, B.J. 2015 Triadic scale interactions in a turbulent boundary layer. *J. Fluid Mech.* **767**, R4.

Ganapathisubramani, B., Hutchins, N., Monty, J.P., Chung, D. & Marusic, I. 2012 Amplitude and frequency modulation in wall turbulence. *J. Fluid Mech.* **712**, 61–91.

Ganapathisubramani, B., Longmire, E.K. & Marusic, I. 2003 Characteristics of vortex packets in turbulent boundary layers. *J. Fluid Mech.* **478**, 35–46.

Hutchins, N. 2014 Large-scale structures in high reynolds number wall-bounded turbulence. In *Progress in Turbulence V*, pp. 75–83. Springer.

Hutchins, N. & Marusic, I. 2007 Evidence of very long meandering features in the logarithmic region of turbulent boundary layers. *J. Fluid Mech.* **579**, 1–28.

Hutchins, N., Monty, J.P., Ganapathisubramani, B., Ng, H.C.H. & Marusic, I. 2011 Three-dimensional conditional structure of a high-reynolds-number turbulent boundary layer. *J. Fluid Mech.* **673**, 255–285.

Jacobi, I & McKeon, BJ 2013 Phase relationships between large and small scales in the turbulent boundary layer. *Experiments in fluids* **54** (3), 1–13.

Kim, K.C. & Adrian, R.J. 1999 Very large-scale motion in the outer layer. *Phys. Fluids* **11** (2), 417–422.

Kline, S.J., Reynolds, W.C., Schraub, F.A. & Runstadler, P.W. 1967 The structure of turbulent boundary layers. *J. Fluid Mech.* **30** (04), 741–773.

Mathis, R., Hutchins, N. & Marusic, I. 2009 Large-scale amplitude modulation of the small-scale structures in turbulent boundary layers. *J. Fluid Mech.* **628**, 311–337.

Mathis, R., Hutchins, N. & Marusic, I. 2011 A predictive inner–outer model for streamwise turbulence statistics in wall-bounded flows. *J. Fluid Mech.* **681**, 537–566.

Mejia-Alvarez, R. & Christensen, K.T. 2010 Low-order representations of irregular surface roughness and their impact on a turbulent boundary layer. *Phys. Fluids* **22** (1), 015106.

Mejia-Alvarez, R. & Christensen, K.T. 2013 Wall-parallel stereo particle-image velocimetry measurements in the roughness sublayer of turbulent flow overlying highly irregular roughness. *Phys. Fluids* **25** (11), 115109.

Mejia-Alvarez, R., Wu, Y. & Christensen, K.T. 2014 Observations of meandering superstructures in the roughness sublayer of a turbulent boundary layer. *Int. J. Heat Fluid Fl.* **48**, 43–51.

Natrajan, V. K. & Christensen, K. T. 2006 The role of coherent structures in subgrid-scale energy transfer within the log layer of wall turbulence. *Phys. Fluids* **18**, 065104.

Ng, H.C.H., Monty, J.P., Hutchins, N., Chong, M.S. & Marusic, I. 2011 Comparison of turbulent channel and pipe flows with varying Reynolds number. *Exp. Fluids* **51** (5), 1261–1281.

Rao, K.N., Narasimha, R. & Narayanan, M.A. 1971 The bursting phenomenon in a turbulent boundary layer. *J. Fluid Mech.* **48** (02), 339–352.

Schlatter, P. & Örlü, R. 2010 Quantifying the interaction between large and small scales in wall-bounded turbulent flows: A note of caution. *Phys. Fluids* **22** (5), 051704.

Wu, Y. & Christensen, K.T. 2007 Outer-layer similarity in the presence of a practical rough-wall topography. *Phys. Fluids* **19** (8), 85108–85108.

Wu, Y. & Christensen, K. T. 2010 Spatial structure of a turbulent boundary layer with irregular surface roughness. *J. Fluid Mech.* **655**, 380–418.